



Fraser, W. B., & Champneys, A. R. (2000). The `Indian rope trick' for a parametrically excited flexible rod : nonlinear and subharmonic analysis.

[Link to publication record in Explore Bristol Research](#)
PDF-document

University of Bristol - Explore Bristol Research

General rights

This document is made available in accordance with publisher policies. Please cite only the published version using the reference above. Full terms of use are available:
<http://www.bristol.ac.uk/pure/about/ebr-terms.html>

Take down policy

Explore Bristol Research is a digital archive and the intention is that deposited content should not be removed. However, if you believe that this version of the work breaches copyright law please contact open-access@bristol.ac.uk and include the following information in your message:

- Your contact details
- Bibliographic details for the item, including a URL
- An outline of the nature of the complaint

On receipt of your message the Open Access Team will immediately investigate your claim, make an initial judgement of the validity of the claim and, where appropriate, withdraw the item in question from public view.

The ‘Indian rope trick’ for a parametrically excited flexible rod; nonlinear and subharmonic analysis

BY W. BARRIE FRASER⁽¹⁾ & ALAN R. CHAMPNEYS⁽²⁾

(1) *School of Mathematics and Statistics, The University of Sydney, NSW 2006, Australia. email: barrief@maths.usyd.edu.au*

(2) *Department of Engineering Mathematics, Queens Building, University of Bristol, Bristol BS8 1TR, UK. email: a.r.Champneys@bris.ac.uk*

Recently Mullin has demonstrated experimentally that an upright column that is longer than its critical length for self-weight buckling can be stabilized by subjecting it to vertical harmonic excitation. This paper extends an earlier linearized analysis of a rod-mechanics model of this set up, to include three-dimensionality, and geometric nonlinearity. The stability of the upright state is then analysed using weakly nonlinear asymptotic expansions in the limit of small-amplitude excitation.

First, the unforced problem is treated, extending the classical result by Greenhill to show that all bifurcations are supercritical. The main results are for the forced problem near the simplest among the potential infinity of dynamic instabilities. These correspond to pure bending modes, and to resonances between a vibration mode of the column and the first harmonic or subharmonic of the drive. The result is to produce an asymptotic description of these instabilities, including information on the stability of dynamically bifurcating states, in terms of the three dimensionless parameters of the problem (bending stiffness and the amplitude and frequency of excitation). A qualitative explanation is offered of why the earlier linearised analysis fails to quantitatively match the experiments.

Keywords: rod mechanics, parametric excitation, inverted pendulum, asymptotic analysis, subharmonic resonance

1. Introduction

It is well known that if a column exceeds a certain critical length it will, when placed upright, buckle under its own weight. Recently, as illustrated in Acheson (1997)[Ch. 12], Tom Mullin has performed experiments on a flexible piece of ‘curtain wire’ (a thin, plastic coated, tightly wound helical metal spring) that is just longer than its critical length. He found that such a wire can be stabilized by parametric excitation, namely by subjecting its bottom support point to a vertical harmonic vibration of appropriate amplitude and frequency. This demonstration was motivated by earlier experiments (Acheson & Mullin 1993) which verify the stabilization by parametric excitation of an inverted system of coupled pendula. A delightfully simple explanation for the case of N coupled pendula was given in Acheson (1993), which extends the result for a single inverted pendulum due originally to Stephenson (1908). However, this theory does not extend to the case $N \rightarrow \infty$ (see Otterbein (1982)) or to

the inclusion of bending stiffness, which together would lead to the problem addressed here. The use of oscillatory excitation to stabilize systems such as inverted pendula is also of interest in control theory, e.g. Weibel & Baillieul (1998). Here, though, we do not consider any feedback or other control effects, just the case of constant sinusoidal vertical forcing. Specifically we shall extend the results in our earlier paper (Champneys & Fraser (2000), henceforth referred to as ‘Part I’) on a parametrically excited continuously flexible column with bending stiffness.

The linearized analysis presented in Part I, which is summarized in the course of the results presented below, is appealing in that it provides a simple lower bound on the product of the excitation frequency and amplitude necessary to stabilize the column. Moreover, this bound can be expressed solely in terms of the ratio of the column’s length to the critical one (eq. (4.18) of Part I). However, in order to match the details of Mullin’s experiment (details of which will appear in (Acheson et al. 2000)) there are two problems with this formula. First, it seems to underestimate the true lower bound by a factor of between 2 and 4. Second, it does not explain the experimental observation of an upper bound on the frequency for stabilization. Whereas the low-frequency instability is associated with the wire simply falling over, the upper one appears to be caused by a dynamic resonance of a higher-order spatial mode of the wire with a harmonic of the drive. The present paper is aimed at addressing these deficiencies by the inclusion of three-dimensional effects, and (most crucially) an asymptotic description of (sub)harmonic resonances.

In §2 the derivation of the equations of motion given in Part I is extended to include the geometrically nonlinear terms. In §3 an asymptotic analysis of static buckling/post-buckling behaviour of these equations is given. The main results are contained in §4 which presents a new asymptotic analysis of the dynamic equations for the parametrically excited column. Finally §5 interprets the consequences of the preceding analysis in understanding Mullin’s experiment, draws conclusions and suggests directions for future work.

2. Mathematical Formulation

Consider an initially straight column with a uniform circular cross-section of radius a , length ℓ and mass density m per unit length (see Figure 1). The column is assumed to be inextensible and to have a linear bending moment versus curvature constitutive relation. The derivation of the equations of motion for such a column was given in Part I where it was argued that the effects of rotary inertia and torsional waves could be neglected in this application with no torsional loading. Here we give only the briefest details of the derivation, paying extra attention to the geometrically nonlinear terms.

(a) Dimensionless equations of motion

The equation of motion of the rod shown in Figure 1, derived in part I, is

$$\eta D^2 \mathbf{R} = (\mathcal{T} \mathbf{R}')' - B \{[(\mathbf{R}'' \cdot \mathbf{R}'') \mathbf{R}]' + \mathbf{R}^{IV}\} - \mathbf{k}. \quad (2.1)$$

Here $\mathbf{R}(s, t)$ is the position vector, with respect to the origin O of an inertial frame, of a material point P on the column axis a distance s along the axis from the bottom of the column at time t , $D(\) = \partial(\)/\partial t$, and $(\)' = \partial(\)/\partial s$, and $\mathcal{T}(s, t)$

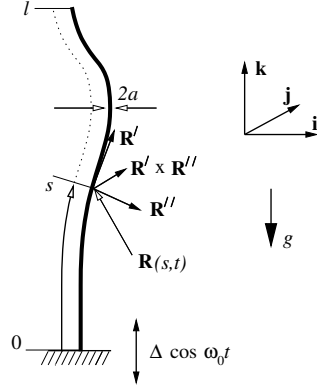


Figure 1. Definition sketch

is the tension in the column at P . Unit vectors \mathbf{i} , \mathbf{j} and \mathbf{k} are the usual basis vectors of the Cartesian frame with origin at O and \mathbf{k} pointing vertically up. The dimensionless variables are defined in terms of dimensional (barred) variables via

$$s = \frac{\bar{s}}{\ell}, \quad \mathbf{R} = \frac{\bar{\mathbf{R}}}{\ell}, \quad t = \omega_0 \bar{t}, \quad \mathcal{T} = \frac{\bar{\mathcal{T}}}{mg\ell}, \quad B = \frac{\bar{B}}{mg\ell^3}, \quad \eta = \frac{\omega_0^2 \ell}{g}, \quad \varepsilon = \frac{\Delta}{\ell},$$

where \bar{B} is the bending stiffness, g is the acceleration due to gravity, ω_0 is the angular frequency of the vertical oscillation of the base of the column and Δ is the amplitude of this oscillation. The inextensibility condition is

$$\mathbf{R}' \cdot \mathbf{R}' = 1. \quad (2.2)$$

The bottom ($s = 0$) end of the column is assumed to be clamped to a device that oscillates vertically. Hence the lower boundary condition is

$$\mathbf{R}(0, t) = \varepsilon \cos t \mathbf{k}, \quad \mathbf{R}'(0, t) = \mathbf{k} \quad \text{at } s = 0. \quad (2.3)$$

The top end of the column is free, which implies the shear force, moment and tension there must vanish, which can be shown to be equivalent to

$$\mathbf{R}''(1, t) = \mathbf{R}'''(1, t) = \mathbf{0}, \quad \mathcal{T}(1, t) = 0. \quad (2.4)$$

Suitable initial conditions are the specification of the position $\mathbf{R}(s, 0)$ and velocity $D\mathbf{R}(s, 0)$, with the tension $\mathcal{T}(s, t)$ then determined by the inextensibility condition.

The model (2.1) and inextensibility condition (2.2) together with these boundary and initial conditions represent a well-posed problem for the position vector $\mathbf{R}(s, t)$ and tension $\mathcal{T}(s, t)$. Note that the nonlinearity comes not from any constitutive law, but from the geometrically nonlinear expression for the bi-normal vector $\mathbf{R}' \times \mathbf{R}''$ about which bending takes place. Note also that the inextensibility condition (2.2) contains no time derivatives, so viewed as an infinite-dimensional dynamical system, the model is an (index 2) differential algebraic equation.

(b) Subtracting out the trivial solution

The vertically straight solution of (2.1), (2.2) subject to (2.3), (2.4) is

$$\mathbf{R}(s, t) = (\varepsilon \cos t + s)\mathbf{k}, \quad \mathcal{T}(s, t) = -(1 - \eta\varepsilon \cos t)(1 - s)$$

In order to investigate its stability and to include the possibility of large lateral deflections of the vertically oscillating column, substitute the following into (2.1):

$$\mathbf{R}(s, t) = (\varepsilon \cos t + s)\mathbf{k} + \mathbf{r}(s, t), \quad T(s, t) = -(1 - \eta\varepsilon \cos t)(1 - s) + T,$$

where \mathbf{r} , and T are not necessarily assumed to be small as they were in Part I. Taking the inextensibility condition (2.2) into account, the result is

$$\eta \{ D^2 \mathbf{r} - \varepsilon \cos t [(1 - s)\mathbf{r}']' \} = -M\mathbf{r} + T'\mathbf{k} + (T\mathbf{r}')' - B[(\mathbf{r}'' \cdot \mathbf{r}'')(\mathbf{k} + \mathbf{r}')]' \quad (2.5)$$

$$2\mathbf{r}' \cdot \mathbf{k} + \mathbf{r}' \cdot \mathbf{r}' = 0, \quad \text{where } M\mathbf{r} := B\mathbf{r}^{IV} + [(1 - s)\mathbf{r}']'. \quad (2.6)$$

The boundary conditions (2.3) and (2.4) become

$$\mathbf{r} = \mathbf{r}' = \mathbf{0}, \quad \text{at } s = 0; \quad \mathbf{r}'' = \mathbf{r}''' = \mathbf{0}, \quad T = 0, \quad \text{at } s = 1. \quad (2.7)$$

This completes the formulation of the nonlinear stability problem.

3. Static post-buckling analysis ($\eta = 0$)

In this section the classical buckling problem for a vertical column under its own weight is extended to determine the immediate post-buckling behaviour. Setting $\eta = 0$ in (2.5), (2.6) results in a problem in which the bending stiffness B is the only dimensionless parameter. Therefore, consider the following perturbation expansion in a small parameter σ which measures distance of B from a bifurcation value B_0 :

$$\left. \begin{aligned} B &= B_0(1 + p\sigma^2), & \mathbf{r}(s) &= \sigma\mathbf{r}_1(s) + \sigma^2\mathbf{r}_2(s) + \sigma^3\mathbf{r}_3(s) + \cdots, \\ T &= \sigma T_1(s) + \sigma^2 T_2(s) + \sigma^3 T_3(s) + \cdots, \end{aligned} \right\}$$

where $p = \pm 1$ and bifurcation values $B = B_0$ are to be determined as part of the solution process. Note the σ^2 dependence in B is due to the reflection symmetry of the problem which dictates that all bifurcations are pitchforks. Now substitute this form into (2.5) and set successive coefficients of σ to zero, to give:

$$M_0\mathbf{r}_1 - T_1'\mathbf{k} = 0, \quad (3.1)$$

$$M_0\mathbf{r}_2 - T_2'\mathbf{k} = -B_0(\mathbf{r}_1'' \cdot \mathbf{r}_1'')'\mathbf{k} + (T_1\mathbf{r}_1')', \quad (3.2)$$

$$M_0\mathbf{r}_3 - T_3'\mathbf{k} = -B_0 [p\mathbf{r}_1^{IV} + 2(\mathbf{r}_1'' \cdot \mathbf{r}_2'')'\mathbf{k} + (\|\mathbf{r}_1''\|^2\mathbf{r}_1')'] + (T_2\mathbf{r}_1' + T_1\mathbf{r}_2')', \quad (3.3)$$

where M_0 is M evaluated at $B = B_0$. The inextensibility condition (2.6)₁ gives

$$\mathbf{k} \cdot \mathbf{r}_1' = 0, \quad \mathbf{k} \cdot \mathbf{r}_2' = -\frac{1}{2}(\mathbf{r}_1' \cdot \mathbf{r}_1'), \quad \mathbf{k} \cdot \mathbf{r}_3' = -(\mathbf{r}_1' \cdot \mathbf{r}_2'), \quad (3.4)$$

with each $\{\mathbf{r}_i(s), T_i(s)\}$, $i = 1, 2, 3$, subject to boundary conditions (2.7).

Consider the $O(\sigma)$ equation (3.1). Taking its scalar product with \mathbf{k} , using the boundary and inextensibility conditions, one finds that $T_1 = 0$, leaving

$$M_0\mathbf{r}_1 := B_0\mathbf{r}_1^{IV} + [(1 - s)\mathbf{r}_1']' = \mathbf{0}. \quad (3.5)$$

As known to Greenhill (1881) this equation, subject to (2.7), has solution

$$\mathbf{r}_1 = \mathbf{u}_k(s) = A_k\psi_k(s)\mathbf{i}, \quad k = 1, 2, 3, \dots \quad (3.6)$$

Here A_k is an unknown amplitude, without loss of generality the vector \mathbf{r}_1 (which must be perpendicular to \mathbf{k}) is orientated in the \mathbf{i} direction, and the eigenfunctions ψ_k may be expressed in terms of a Bessel function $J_{-1/3}$ via $\psi_k(0) = 0$ and

$$\psi'_k(s) = \sqrt{\frac{1-s}{N_k}} J_{-1/3} \left(\frac{2}{3} \Lambda_k^{-\frac{1}{2}} (1-s)^{\frac{3}{2}} \right), \quad N_k = \int_0^1 \left[\sqrt{1-s} J_{-1/3} \left(\frac{2}{3} \Lambda_k^{-\frac{1}{2}} (1-s)^{\frac{3}{2}} \right) \right]^2 ds. \quad (3.7)$$

The corresponding eigenvalues $B_0 = \Lambda_k$ are the zeros of $J_{-1/3} \left(\frac{2}{3} B_0^{-\frac{1}{2}} \right)$; $\Lambda_1 = 0.127594$, $\Lambda_2 = 0.017864$, $\Lambda_3 = 0.0067336$, $\Lambda_4 = 0.0003503$, $\Lambda_5 = 0.0002142$, \dots . Equation (3.5) is self-adjoint, the eigenfunctions satisfy the orthogonality relations

$$\left. \begin{aligned} \int_0^1 \mathbf{u}_k \cdot \mathbf{u}_j^{IV} ds &= - \int_0^1 \mathbf{u}'_k \cdot \mathbf{u}''_j ds = \int_0^1 \mathbf{u}''_k \cdot \mathbf{u}'_j ds = \\ \int_0^1 [(1-s)\mathbf{u}'_k]' \cdot \mathbf{u}_j ds &= \int_0^1 (1-s)\mathbf{u}'_k \cdot \mathbf{u}'_j ds = 0 \end{aligned} \right\} \text{for all } k \neq j. \quad (3.8)$$

and they have been normalized so that $\int_0^1 (\psi'_k)^2 ds = 1$.

The solution of prime interest in this paper is the one that bifurcates from the largest eigenvalue $\Lambda_1 = 0.127594$, corresponding to eigenfunction $\mathbf{u}_1(s)$ above. This is because $B = \Lambda_1 := B_{cr}$ corresponds to the critical value of dimensionless bending stiffness below which a column is unstable (the '*greatest height consistent with stability*' Greenhill (1881)), see Part I §3(e). Thus each lower eigenvalue Λ_k with $k > 1$ corresponds upon decreasing B to a further loss of stability from an already unstable state. Hence let us take

$$\mathbf{r}_1(s) = \mathbf{u}_1(s), \quad T_1 = 0, \quad \text{and} \quad B_0 = \Lambda_1 = 0.127594, \quad (3.9)$$

where $\mathbf{u}_1(s)$ is given by (3.6) with the amplitude A_1 to be determined. The inextensibility conditions (3.4) now become

$$\mathbf{k} \cdot \mathbf{u}'_1 = 0, \quad \mathbf{k} \cdot \mathbf{r}'_2 = -\frac{1}{2}(\mathbf{u}'_1 \cdot \mathbf{u}'_1), \quad \mathbf{k} \cdot \mathbf{r}'_3 = -(\mathbf{u}'_1 \cdot \mathbf{r}'_2). \quad (3.10)$$

Now consider the $O(\sigma^2)$ equation (3.2) after substitution of (3.9):

$$\Lambda_1 \mathbf{r}_2^{IV} + [(1-s)\mathbf{r}'_2]' - T'_2 \mathbf{k} = -\Lambda_1 (\mathbf{u}''_1 \cdot \mathbf{u}'_1)' \mathbf{k}, \quad (3.11)$$

To find an expression for T_2 , form the scalar product (3.11) with \mathbf{k} , using the inextensibility condition (3.10)₂, to obtain an equation for T'_2 which can be integrated, the integration constant being zero due to the boundary conditions (2.7):

$$T_2(s) = \Lambda_1 (\mathbf{u}''_1 \cdot \mathbf{u}'_1) - \frac{1}{2} \Lambda_1 (\mathbf{u}'_1 \cdot \mathbf{u}'_1)'' - \frac{1}{2} (1-s) (\mathbf{u}'_1 \cdot \mathbf{u}'_1). \quad (3.12)$$

Equation (3.11) now reduces to

$$M_0 \mathbf{r}_2 = \Lambda_1 \mathbf{r}_2^{IV} + [(1-s)\mathbf{r}'_2]' = \frac{1}{2} \{ \Lambda_1 (\mathbf{u}'_1 \cdot \mathbf{u}'_1)''' + [(1-s)\mathbf{u}'_1 \cdot \mathbf{u}'_1]' \} \mathbf{k}, \quad (3.13)$$

where all terms on the right-hand side are now known functions. The solvability condition for (3.13) is that the right-hand side be orthogonal to $\mathbf{u}_1(s)$. Only the

particular integral is of interest as any contribution from the solution (3.7) of the homogeneous equation can be absorbed into the $O(1)$ term \mathbf{r}_1 . The particular solution is $\mathbf{r}_2 = f_2(s)\mathbf{k}$, where $f_2(s)$ satisfies

$$M_0 f_2 = -\frac{A_1^2}{2} \{ \Lambda_1 [(\psi_1')^2]''' + [(1-s)(\psi_1')^2]' \}.$$

A calculation using (3.8) shows that the right-hand-side of this equation is orthogonal to $\mathbf{u}_1(s)$ as required and that the particular integral solution is $f_2' = -\frac{1}{2}(A_1 \psi_1')^2$.

Now go to $O(\sigma^3)$. Since the solution $\mathbf{r}_2(s)$ and its derivatives are in the \mathbf{k} direction, and $\mathbf{r}_1'(s)$ is perpendicular to \mathbf{k} , the inextensibility condition (3.13)₃ reduces to $\mathbf{k} \cdot \mathbf{r}_3' = 0$. The tension perturbation T_3 is then found to be zero from the \mathbf{k} -component of (3.3). When all known terms are substituted into (3.3) it reduces to

$$M_0 \mathbf{r}_3 = \Lambda_1 \mathbf{r}_3^{IV} + [(1-s)\mathbf{r}_3']' = -p\Lambda_1 \mathbf{u}_1^{IV} - \Lambda_1 [(\mathbf{u}_1'' \cdot \mathbf{u}_1'')' + (T_2 \mathbf{u}_1')'].$$

The right-hand side is now known, up to the unknown sign p and amplitude A_1 of \mathbf{u}_1 , which are determined by the solvability (orthogonality) condition

$$p\Lambda_1 \int_0^1 (\mathbf{u}_1^{IV} \cdot \mathbf{u}_1) ds = \int_0^1 \{ (T_2 \mathbf{u}_1')' - \Lambda_1 [(\mathbf{u}_1'' \cdot \mathbf{u}_1'')'] \} \cdot \mathbf{u}_1 ds.$$

Integration by parts twice and substitution for T_2 from (3.12) gives

$$p\Lambda_1 \int_0^1 (\mathbf{u}_1'' \cdot \mathbf{u}_1'') ds = \frac{1}{2} \int_0^1 \{ (1-s)(\mathbf{u}_1' \cdot \mathbf{u}_1')^2 - \Lambda_1 [(\mathbf{u}_1' \cdot \mathbf{u}_1')']^2 \} ds.$$

Substitution of $\mathbf{u}_1(s)$ from (3.6), then gives an expression for p and A_1 :

$$\frac{p\Lambda_1}{A_1^2} = K_1 := \left(\frac{1}{2} \int_0^1 \{ (1-s)(\psi_1')^4 - 4\Lambda_1 (\psi_1' \psi_1'')^2 \} ds \right) / \int_0^1 (\psi_1'')^2 ds, \quad (3.14)$$

where $\Lambda_1 = 0.127594$, and $\psi_1(s)$ is given by (3.7) with $N_1 = 2.795394\dots$

Evaluation of the integrals in (3.14) using Maple, reveals that $K_1 = -.0239242$; hence $p = -1$ and $A_1 = 2.309388$. The final post-bifurcation result is therefore that, for $B = 0.127954(1 - \sigma^2)$, with $|\sigma| \ll 1$, the centreline is

$$\mathbf{R}(s) = \sigma[(2.309\dots)\psi_1(s)] \mathbf{i} + \left(s - \frac{\sigma^2}{2}(2.309\dots)^2 \int_0^s \psi_1'(z)^2 dz \right) \mathbf{k} + \mathcal{O}(\sigma^3),$$

where ψ_1 is defined by (3.7). This bifurcation is the right-hand one depicted in Figure 2. Specifically it shows that as bending stiffness is *decreased* through $B = B_{cr}$ (to values of B just slightly less than B_{cr}) the vertically upright configuration ($\sigma = 0$) becomes unstable and the column assumes a stable equilibrium position displaced from the vertical ($|\sigma| > 0$).

Before proceeding to a dynamic analysis, note that the above post-buckling analysis is easily repeated at each of the other static bifurcation points $B = \Lambda_k$, $k > 1$, by replacement of the subscript 1 on ψ_1 , etc. by k . A remarkable fact, found by numerical evaluation of the integrals K_k for $k > 1$ is that $p < 0$ in each case and, given the choice of normalization, that $A_k = A_1$. Hence each bifurcation is a supercritical pitchfork and when appropriately rescaled (recall that σ^2 represents the percentage change of B from its bifurcation value) the quadratic bifurcating curves are identical. The first three curves are plotted in Figure 2.

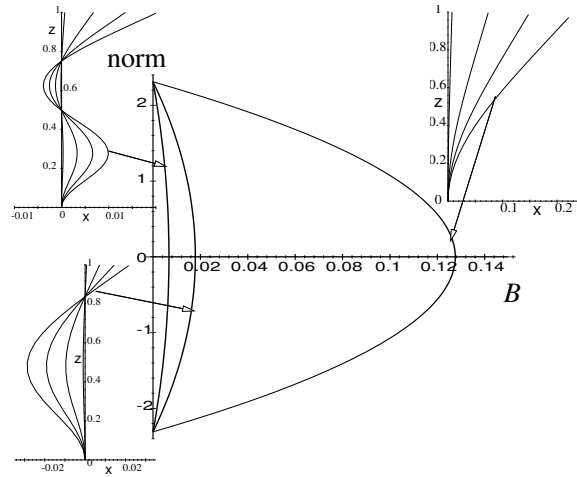


Figure 2. Weakly nonlinear static post-buckling analysis showing the first three bifurcations. The norm in the ordinate is the L_2 -norm of $\mathbf{r}' \cdot \mathbf{i}$. All curves are depicted beyond the region of validity of the analysis. The insets show the corresponding bifurcating modes at $\sigma = 0.01, 0.1, 0.2$ and 0.3 .

4. Multiple-Timescale Dynamic Asymptotic Analysis

(a) Linear Modal Analysis

Now consider $\eta > 0$ and let us briefly recall the analysis from Part I of the forced and unforced dynamic problem obtained from the linearized version of (2.5). It was assumed, without loss of generality, that $\mathbf{r}(s, t) = u(s, t)\mathbf{i}$ so that the linearized equation is [cf. Part I Eq. (3.11)]

$$\eta D^2 u = -(1 - \eta \varepsilon \cos t)[(1 - s)u']' - B u^{IV},$$

The results are summarized qualitatively in Figure 3. Here the $\lambda_n(B)$ $n = 1, 2, \dots$ represent the vibration frequencies of the solution to the unforced ($\varepsilon = 0$) problem

$$u(s, t) = \sum \phi_n(s; B) \left\{ A_n \cos \left[\sqrt{\lambda_n/\eta} t \right] + B_n \sin \left[\sqrt{\lambda_n/\eta} t \right] \right\},$$

where the $\phi_n(s; B)$ are the eigenfunctions of $M\phi_n - \lambda_n\phi_n = 0$, subject to the boundary conditions (2.7), where M is given in (2.6)₂. The eigenfunctions and eigenvalues are related to the static ones via $\lambda_k(B = \Lambda_k) = 0$, and $\phi_k(s; B = \Lambda_k) = \psi_k$, and satisfy the orthogonality relations (for fixed B)

$$\int \phi_m \phi_n ds = \int [M\phi_m] \phi_n ds = 0, \quad \text{with } n \neq m, \quad \text{and } \lambda_m \neq \lambda_n.$$

Unlike the static eigensolutions, the ϕ_n are not expressible in closed form. Numerically the ϕ_n have the same basic mode shapes as the ψ_n ; and $\lambda_n(B)$ is approximately a linear function for each n (see Fig. 2 of Part I).

Moreover, in Part I section 5, it was shown via infinite-dimensional Floquet theory that at each B -value such that $\lambda_j(B) = \eta(\frac{i}{2})^2$ for some non-negative integer i and positive integer j , there is the root point of an (Arnol'd or Mathieu) instability

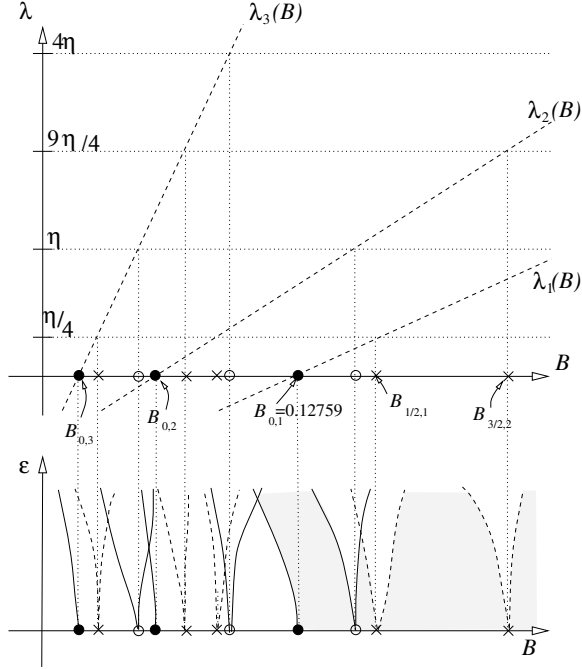


Figure 3. Summarizing the results from Part I, see text for details. The shaded regions correspond to the where the vertical solution is stable. Solid lines correspond to Floquet multipliers +1 and dashed lines to multipliers -1.

tongue in the (ε, B) -plane, as depicted qualitatively in the lower part of Figure 3. Here $i/2$ counts the temporal harmonic and j the spatial mode number. The B -values of these roots are labelled $B_{i/2,j}$, where by definition $B_{0,j} = \Lambda_j$. Note that the relative location of the tongues is highly η -dependent. Note also that Figure 3 is a caricature and in reality, as confirmed by numerical computation in Part I, those tongues corresponding to $i > 1$ are remarkably narrow.

(b) *The multiple-timescale asymptotic analysis*

In Part I, section 4 a two-timing asymptotic analysis of the linearized problem was undertaken in the vicinity of $B = B_{cr} = B_{0,1}$. This confirmed that the primary resonance curve emanating from this point bends back to the left as depicted in Figure 3 (although see the caveat presented in §4(c) below). This shows that for small ε there is a short range of B -values at which a statically unstable rod ($B < B_{0,1}$) can be stabilized; the ‘Indian rope trick’. In §4(c) below, this *lower* bound on B (near $B_{0,1}$) for stability is extended to a weakly nonlinear and three-dimensional analysis in the spirit of §3 above. §4(d),(e) then goes on to use the two-timscale asymptotic methods to determine approximations in the (ε, B) -plane to the Mathieu tongues near $\varepsilon = 0$ for the simplest dynamical resonance points, $B = B_{1/2,j}$ and $B_{1,j}$, corresponding to the first subharmonic and harmonic instabilities. The hope is that these will provide an *upper* bound on B for stability, as suggested by Mullin’s experiments.

Before giving the three separate asymptotic analyses, let us construct a general

asymptotic expansion involving two slow timescales $\tau_1 = \varepsilon t$ and $\tau_2 = \varepsilon^2 t$. Timescale τ_1 is required to obtain a distinguished limit for the fundamental resonance near B_{cr} and for subharmonic resonance. Time scale τ_2 is required for the case of harmonic resonance. Thus, consider the following expansions (cf. Kevorkian & Cole (1981)[p.152]):

$$\left. \begin{aligned} B &= B_0 + \varepsilon B_1 + \varepsilon^2 B_2 + \cdots, \\ \mathbf{r}(s, t) &= \varepsilon \mathbf{r}_1(s, t, \tau_1, \tau_2) + \varepsilon^2 \mathbf{r}_2(s, t, \tau_1, \tau_2) + \varepsilon^3 \mathbf{r}_3(s, t, \tau_1, \tau_2) + \cdots, \\ T(s, t) &= \varepsilon T_1(s, t, \tau_1, \tau_2) + \varepsilon^2 T_2(s, t, \tau_1, \tau_2) + \varepsilon^3 T_3(s, t, \tau_1, \tau_2) + \cdots. \end{aligned} \right\}$$

When these expansions are substituted into (2.5) and the coefficients of powers of ε in the resulting equations are set to zero, we obtain

$$\eta \frac{\partial^2 \mathbf{r}_1}{\partial t^2} + M_0 \mathbf{r}_1 - T_1' \mathbf{k} = \mathbf{0}, \quad (4.1)$$

$$\eta \frac{\partial^2 \mathbf{r}_2}{\partial t^2} + M_0 \mathbf{r}_2 - T_2' \mathbf{k} = \eta \cos t L \mathbf{r}_1 + (T_1 \mathbf{r}_1')' - B_0 (\|\mathbf{r}_1''\|^2)' \mathbf{k} - B_1 \mathbf{r}_1^{IV} - 2\eta \frac{\partial^2 \mathbf{r}_1}{\partial \tau_1 \partial t} \quad (4.2)$$

$$\begin{aligned} \eta \frac{\partial^2 \mathbf{r}_3}{\partial t^2} + M_0 \mathbf{r}_3 - T_3' \mathbf{k} &= \eta \cos t L \mathbf{r}_2 + (T_1 \mathbf{r}_2' + T_2 \mathbf{r}_1')' - 2B_0 (\mathbf{r}_1' \cdot \mathbf{r}_2'')' \mathbf{k} \\ &- B_0 [\|\mathbf{r}_1''\|^2 \mathbf{r}_1']' - B_1 \mathbf{r}_2^{IV} - B_2 \mathbf{r}_1^{IV} - 2\eta \frac{\partial^2 \mathbf{r}_1}{\partial \tau_2 \partial t} - \eta \frac{\partial^2 \mathbf{r}_1}{\partial \tau_1^2} - 2\eta \frac{\partial^2 \mathbf{r}_2}{\partial \tau_1 \partial t} \end{aligned} \quad (4.3)$$

where $L\mathbf{r} = [(1-s)\mathbf{r}']'$ and M_0 was defined previously. The inextensibility condition again yields (3.4), and the $\mathbf{r}_n(s, t, \tau_1, \tau_2)$ are each subject to the boundary conditions (2.7).

(c) *The first pure bending mode near $B = B_{cr}$; the 'falling-over' instability*

In this case $B_0 = B_{cr}$ and the $O(\varepsilon)$ solution is assumed to be the fundamental buckling mode with its amplitude dependent only on the slow time variables. Thus, the solution of equation (4.1) is taken to be

$$T_1 = 0, \quad \mathbf{r}_1(s, t, \tau_1, \tau_2) = [f(\tau_1, \tau_2)\mathbf{i} + g(\tau_1, \tau_2)\mathbf{j}] \psi_1(s) := \mathbf{F}\psi_1(s), \quad (4.4)$$

which satisfies the inextensibility condition (3.4)₁. For stability, the functions f and g must be bounded as $\tau_1, \tau_2 \rightarrow \infty$. The inextensibility condition (3.4)₂ becomes

$$\mathbf{k} \cdot \mathbf{r}_2' = -\frac{1}{2} \|\mathbf{F}\|^2 (\psi_1')^2. \quad (4.5)$$

The $O(\varepsilon^2)$ equation.

When (4.4) is substituted into the $O(\varepsilon^2)$ equation (4.2), the result is

$$\eta \frac{\partial^2 \mathbf{r}_2}{\partial t^2} + M_0 \mathbf{r}_2 - T_2' \mathbf{k} = \{\eta \cos t L \psi_1(s) - B_1 \psi_1'\} \mathbf{F} - B_0 \|\mathbf{F}\|^2 [(\psi_1'')^2]' \mathbf{k}. \quad (4.6)$$

As before T_2 is found by forming the scalar product of this equation with \mathbf{k} ; thus

$$T_2 = -\|\mathbf{F}\|^2 \left\{ B_0 \left[\frac{1}{2} [(\psi_1'')^2]'' - (\psi_1'')^2 \right] + \frac{1}{2} (1-s)(\psi_1')^2 \right\}. \quad (4.7)$$

Note from (4.5) that $\mathbf{k} \cdot \mathbf{r}_2$ does not depend on the fast time t . When this result is substituted back into (4.6) the solution for \mathbf{r}'_2 is found to be

$$\mathbf{r}'_2(s, t, \tau_1, \tau_2) = [F'_0(s) + \cos t F'_1(s)] \mathbf{F} - \frac{1}{2} \|\mathbf{F}\|^2 (\psi'_1)^2 \mathbf{k},$$

where $F_0(s)$, $F_1(s)$ satisfy the ordinary differential equations

$$M_0 F_0 = -B_1 \psi_1^{IV}, \quad M_0 F_1 - \eta F_1 = \eta L \psi_1(s). \quad (4.8)$$

since the right-hand side of the first equation above is not orthogonal to the eigenfunction ψ_1 of the operator on the left, we must choose $B_1 = 0$.

The dependence of the amplitude functions f and g on τ_1 is determined by a solvability condition for the component of the $O(\varepsilon^3)$ equation that is perpendicular to \mathbf{k} . Let \mathbf{u}_3 be such a component of \mathbf{r}_3 ($\mathbf{u}_3 \cdot \mathbf{k} = 0$) and substitute the above solutions into (4.3) to obtain the following equation for \mathbf{u}_3 :

$$\begin{aligned} \eta \frac{\partial^2 \mathbf{u}_3}{\partial t^2} + M_0 \mathbf{u}_3 = & -\eta \psi_1 \frac{\partial^2 \mathbf{F}}{\partial \tau_1^2} + \frac{1}{2} \eta \cos 2t L F_1(s) \mathbf{F} + 2\eta \sin t F_1(s) \frac{\partial \mathbf{F}}{\partial \tau_1} \\ & + \left\{ \frac{1}{2} \eta L F_1 - B_2 \psi_1^{IV} - \frac{1}{2} \left[B_0 (\psi_1'^2)'' \psi_1' + (1-s) \psi_1'^3 \right]' \|\mathbf{F}\|^2 \right\} \mathbf{F} \end{aligned}$$

The particular integral of this equation is

$$\mathbf{u}_3 = \mathbf{G}_0(s, \tau_1, \tau_2) + \cos 2t G_1(s, \tau_1, \tau_2) \mathbf{F} + \sin t G_2(s, \tau_1, \tau_2) \frac{\partial \mathbf{F}}{\partial \tau_1},$$

$$\text{where } M_0 G_1 - 4\eta G_1 = \frac{1}{2} \eta L F_1, \quad M_0 G_2 - \eta G_2 = 2\eta F_1 \quad \text{and}$$

$$M_0 \mathbf{G}_0 = \left\{ \frac{1}{2} \eta L F_1 - B_2 \psi_1^{IV} - \frac{1}{2} \left[B_0 (\psi_1'^2)'' \psi_1' + (1-s) \psi_1'^3 \right]' \|\mathbf{F}\|^2 \right\} \mathbf{F} - \eta \psi_1 \frac{\partial^2 \mathbf{F}}{\partial \tau_1^2}, \quad (4.9)$$

with each of the functions $G_n(s, \tau_1, \tau_2)$ satisfying the boundary conditions (2.7).

Finally, the condition for the existence of the particular integral of (4.9) gives equations for $\mathbf{F} = f\mathbf{i} + g\mathbf{j}$ as a function of τ_1 :

$$\frac{\partial^2 f}{d\tau_1^2} + P f + Q(f^2 + g^2) f = 0, \quad \frac{\partial^2 g}{d\tau_1^2} + P g + Q(f^2 + g^2) g = 0, \quad (4.10)$$

$$\begin{aligned} P &= \left(\int_0^1 \left[B_2 \psi_1^{IV} - \frac{1}{2} \eta L F_1 \right] \psi_1 ds \right) / \mathcal{A}, \quad \text{where } \mathcal{A} = \eta \int_0^1 \psi_1^2 ds \quad (4.11) \\ Q &= \frac{-1}{2\mathcal{A}} \int_0^1 \{ B_0 [(\psi_1')^2]'' + (1-s)(\psi_1')^2 \} (\psi_1')^2 ds = -\frac{K_1}{\mathcal{A}} \int_0^1 (\psi_1'')^2 ds, \end{aligned}$$

and K_1 is given by (3.14). To obtain these expressions for P and Q , the terms in the numerators have been simplified by integration by parts. The τ_2 dependence is determined at $O(\varepsilon^4)$ but does not add any significant behaviour.

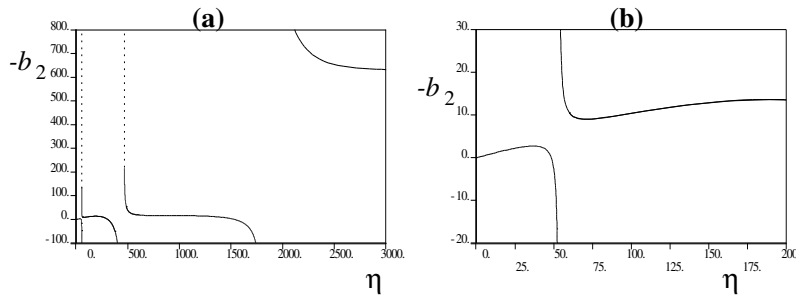


Figure 4. Numerical evaluation of the coefficient $B_2 = b_2$ for which $P = 0$. Panel (b) shows a blow up of (a) for small η

Consider now the amplitude equations (4.10). They can be written more compactly in complex form after defining $z = f + ig$ from which it is apparent that they are rotation invariant and completely integrable, and satisfy the circularly symmetric unforced Duffing equation $z'' + Pz + Q\|z\|^2 z = 0$. The origin $z = 0$ is stable for $P > 0$ and unstable for $P < 0$. Hence the stability boundary is given by those values of $B_2 := b_2(\eta)$ for which P given by (4.11) is zero. Note that P is the same as the coefficient $-\alpha^2$ found in the linearized analysis in Part I (eq. (4.12) of that paper) where real values of α represent the vibration frequency about the zero solution. Note that these linear vibrations include circular modes, which can be seen by setting $z = Re^{i\theta(t)}$ with $R = \text{const.}$ from which we obtain $\dot{\theta}^2 = P + QR^2$. Nonlinearly, this relationship gives the frequency of rotating ‘relative equilibria’ as a function of R , η and B .

In Part I, the stability boundary $b_2(\eta)$ was found to be sensitive to η . In Figure 4 we present more details of this result which was obtained by numerical evaluation of the integral (4.11) after solving the boundary-value problems (4.8)₂ using AUTO (Doedel et al. 1997). Note that the curve has an asymptote for small η of $b_2 \approx -C(\eta)\eta$ where $C \approx 0.1$, which leads to the simple lower stability bound given in Part I. However, as is more apparent here where η rather than $\delta = 1/\eta$ is the frequency parameter, for larger η this asymptotic curve while still correct ‘on average’ is punctuated by a series of singularities (the first three near $\eta = 53.3$, 460.7 and 1813.5). In §5 we shall give an explanation of these singularities, which were erroneously put down to secondary ‘bifurcations’ in Part I.

Consider now, the *nonlinear* implications of these stability results. For simplicity, bearing in mind the rotation symmetry, we shall restrict ourselves to planar modes in the invariant plane $g = 0$, leaving the planar Duffing equation (4.10)₁ with $g = 0$. Since $K_1 < 0$ then $Q > 0$ and, if $B > b_2(\eta)$, then all the phase-plane trajectories are periodic and the origin is a centre. Hence linear stability implies nonlinear stability. See Figure 5(a). If, on the other hand, $B_2 < b_2(\eta)$ then $P < 0$ then the origin becomes a saddle flanked by the symmetrically-opposite bifurcated stable equilibria corresponding to the fundamental static mode ψ_1 . See Figure 5(b). Hence linear instability does not necessarily imply nonlinear instability, since small perturbations will form oscillations about one or other of the leaning-over equilibrium states. With the addition of small damping, this implies that under quasi-static reduction in B (which is experimentally realisable by increasing the length of the rod), a stable

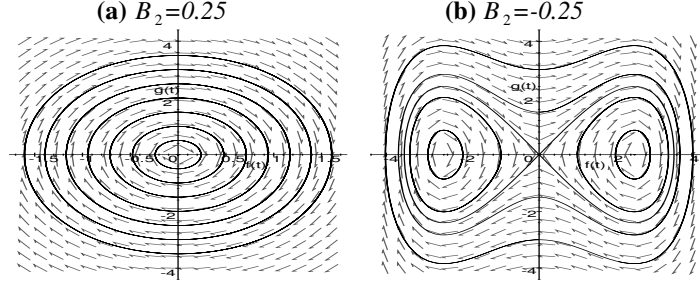


Figure 5. Showing the phase-plane of the slow-time equation (4.10) with $g = 0$ and $\delta = 1$ so that $Q = 0.2971$, and: (a) $B_2 = 0.25 > b_2$, implying $P = 4.3559$; (b) $B_2 = -0.25 < b_2$, implying $P = -1.8532$.

one-sided leaning state would be observed before any gross instability of the upside down position sets in.

Finally note that, up to numerical evaluation of coefficients P and Q , the above analysis works near $B = B_{0,j}$ for $j = 2, 3, \dots$, by simply replacing ψ_1 by ψ_j .

(d) *Subharmonic resonance in the neighbourhood of $B = B_{1/2,j}$*

In the case of resonance where the vibration frequency of mode ϕ_j is half that of the drive, it will transpire that the instability boundary is fully determined by the $O(\varepsilon^2)$ equations which are independent of timescale τ_2 . Analysis of the $O(\varepsilon^3)$ equations then leads to expressions for the amplitude of the bifurcating solutions, but does not alter the leading order expression for the boundary itself. For brevity we shall omit the $O(\varepsilon^3)$ analysis, and hence set $\tau_1 = \tau$ in this subsection. Thus we set $B_0 = B_{1/2,j}$ and take the solution to the $O(\varepsilon)$ equation (4.1) to be $T_1 = 0$ and

$$\mathbf{r}_1 = [f(\tau)\mathbf{m}_{1/2} + 2g(\tau)\dot{\mathbf{m}}_{1/2} + h(\tau)\mathbf{n}_{1/2} + 2k(\tau)\dot{\mathbf{n}}_{1/2}] \phi(s) \equiv \mathbf{N}_{1/2}(t, \tau_1, \tau_2)\phi(s). \quad (4.12)$$

Here, the unit vectors \mathbf{m}_q and \mathbf{n}_q (with $q = 1/2$) are given by

$$\mathbf{m}_q(t) = \mathbf{i} \cos qt + \mathbf{j} \sin qt, \quad \mathbf{n}_q(t) = \mathbf{i} \cos qt - \mathbf{j} \sin qt. \quad (4.13)$$

Also $\phi(s)$ is the solution of $M_0\phi - \frac{q}{4}\phi \equiv B_{1/2,j}\phi^{IV} + L\phi - \frac{q}{4}\phi = 0$, subject to the usual boundary conditions. The amplitude functions $f(\tau)$, $g(\tau)$, $h(\tau)$ and $k(\tau)$ will be determined by the $O(\varepsilon^2)$ equations.

Note that the general notation for the vectors \mathbf{m}_q and \mathbf{n}_q , to be used in §4(e) also, defines vectors which rotate around the \mathbf{k} -axis at the appropriate (sub)harmonic frequency. They have the following properties:

$$\left. \begin{aligned} \mathbf{k} \cdot \mathbf{m}_q &= 0, & \frac{d\mathbf{m}_q}{dt} &\equiv \dot{\mathbf{m}}_q = q\mathbf{k} \times \mathbf{m}_q, & \text{and} & & \ddot{\mathbf{m}}_q &= -q^2\mathbf{m}_q, \\ \mathbf{k} \cdot \mathbf{n}_q &= 0, & \frac{d\mathbf{n}_q}{dt} &\equiv \dot{\mathbf{n}}_q = q\mathbf{k} \times \mathbf{n}_q, & \text{and} & & \ddot{\mathbf{n}}_q &= -q^2\mathbf{n}_q. \end{aligned} \right\} \quad (4.14)$$

Note that planar motions are given with respect to bases $\mathbf{m}_q \pm \mathbf{n}_q$.

When (4.12) is substituted into the $O(\varepsilon^2)$ equation the result is

$$\begin{aligned} \eta \frac{\partial^2 \mathbf{r}_2}{\partial t^2} + M_0 \mathbf{r}_2 - T_2' \mathbf{k} &= \frac{1}{2} \eta \left[f \mathbf{m}_{3/2} + \frac{2}{3} g \dot{\mathbf{m}}_{3/2} + h \mathbf{n}_{3/2} + \frac{2}{3} k \dot{\mathbf{n}}_{3/2} \right] L \phi \\ - 2\eta \left[\frac{df}{d\tau} \dot{\mathbf{m}}_{1/2} - \frac{1}{4} \frac{dg}{d\tau} \mathbf{m}_{1/2} + \frac{dh}{d\tau} \dot{\mathbf{n}}_{1/2} - \frac{1}{4} \frac{dk}{d\tau} \mathbf{n}_{1/2} \right] \phi &- B_{1/2,n} F(t, \tau) [(\phi'')^2]' \mathbf{k} \\ &+ \frac{1}{2} \eta [f \mathbf{n}_{1/2} - 2g \dot{\mathbf{n}}_{1/2} + h \mathbf{m}_{1/2} - 2k \dot{\mathbf{m}}_{1/2}] L \phi - B_1 \mathbf{N}_{1/2} \phi^{IV}, \end{aligned} \quad (4.15)$$

where $F(t, \tau) = (f^2 + g^2 + h^2 + k^2) - 2(fk + hg) \sin t + 2(fh - gk) \cos t$.

Also, by the inextensibility condition, $\mathbf{k} \cdot \mathbf{r}_2' = F(t, \tau) \Phi''(s)$ where $\Phi(s)$ satisfies the ordinary differential equation

$$\Phi''(s) = -\frac{1}{2}(\phi')^2, \quad \text{subject to } \Phi'(0) = \Phi(1) = 0. \quad (4.16)$$

The tension T_2 is found from the \mathbf{k} component of eq. (4.15) to be

$$T_2 = \eta \frac{\partial^2 F}{\partial t^2} \Phi(s) + F(t, \tau) \mathcal{M} \Phi(s) + B_{1/2,n} F(t, \tau) (\phi'')^2, \quad (4.17)$$

where $\mathcal{M} \Phi \equiv B_{1/2,n} \Phi^{IV} + (1-s) \Phi''$.

The solvability condition for (4.15) is that the resonant terms on the right-hand side be orthogonal to $\phi(s)$, which, in components of \mathbf{m} , $\dot{\mathbf{m}}$, \mathbf{n} and $\dot{\mathbf{n}}$, gives

$$\left. \begin{aligned} \frac{dg}{d\tau} + \alpha h - \beta B_1 f &= 0, & 2 \frac{df}{d\tau} + \alpha k + \beta B_1 g &= 0, \\ \frac{dk}{d\tau} + \alpha f - \beta B_1 h &= 0, & 2 \frac{dh}{d\tau} + \alpha g + \beta B_1 k &= 0, \end{aligned} \right\} \quad (4.18)$$

$$\alpha = \int_0^1 \phi L \phi ds / \int_0^1 \phi^2 ds, \quad \text{and} \quad \beta = 2 \int_0^1 (\phi'')^2 ds / \eta \int_0^1 \phi^2 ds.$$

Note that for this resonance, the lowest order amplitude equations (4.18) are linear and hence we can without loss of generality at this stage, consider only planar motions in the (\mathbf{i}, \mathbf{k}) -plane by setting $f = h$, $g = k$. The condition for stability of the trivial equilibrium can then be obtained by eliminating f (or g) from the equations so obtained to give $\frac{d^2}{d\tau^2} g + \frac{1}{2}(B_1^2 \beta^2 - \alpha^2)g = 0$. The solution of this equation will be periodic, giving stability of the trivial solution provided $B_1^2 > (b_1^{(j)})^2 := \alpha^2 / \beta^2$. This determines the approximately linear boundaries of the Arnol'd tongue emanating from the root $B = B_{1/2,j}$ of the (ε, B) -plane:

$$B = B_{1/2,j} \pm \varepsilon b_1^{(j)} + \mathcal{O}(\varepsilon^2), \quad \text{where} \quad b_1^{(j)} = \frac{\eta}{2} \int_0^1 \phi L \phi ds / \int_0^1 \phi''^2 ds \quad (4.19)$$

Figure 6 shows the numerical computation of the integral defining $b_1^{(j)}$ (depicted as an absolute value) together with the value of $B_{1/2,j}$ obtained by solving the eigenvalue problem for the linear boundary-value-problem. Note the striking closeness to linearity of the dependence of both quantities with η (note that b_1 depends nonlinearly on η since ϕ does). Figure 7 shows that these asymptotic formulae agree well

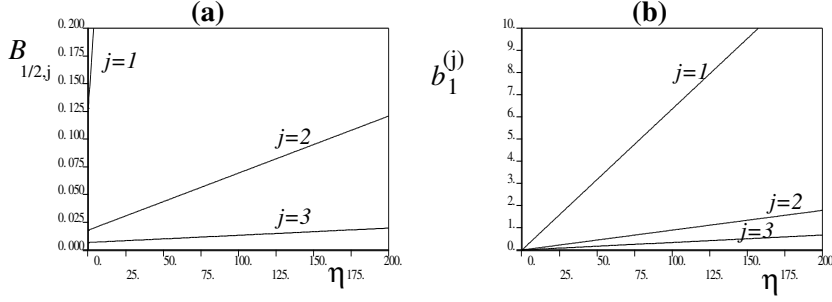


Figure 6. Numerically computed curves $B_{1/2,j}$ and $b_1^{(j)}$ against η , for $j = 1, 2, 3$.

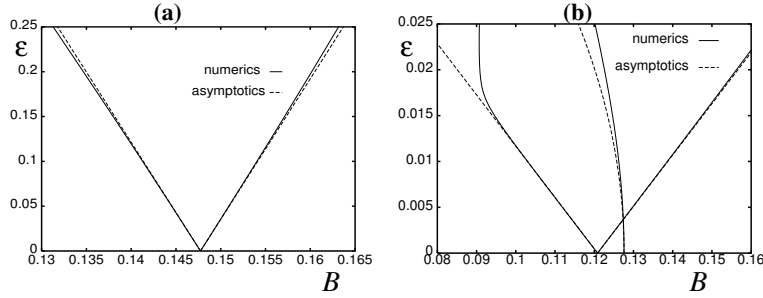


Figure 7. Comparison between numerics and asymptotics for the $(1/2, j)$ -resonance tongue: (a) with $\eta = 1$ and $j = 1$; and (b) with $\eta = 200$ and $j = 2$. The latter value was chosen to illustrate how the resonance interacts with the pure bending mode, whose instability boundary calculated both asymptotically and numerically is also depicted

with the corresponding numerically computed stability boundaries (all such computations in this paper were obtained with the numerical Floquet theory presented in Part I with $N = 4$).

Note that from (4.18), it is possible to distinguish between the dynamic mode corresponding to the left and right instability boundaries in (4.19). That which has $B_1 = +b_1^{(j)}$ corresponds to solutions like $f(\tau) \cos(t/2)$ which have maximum lateral deflection at the top of the vertical excitation, and zero deflection at the bottom. Such motion has been described as ‘nodding’ in Acheson (1995), for the analogous motion of a rigid pendulum. In contrast, those solutions that bifurcate from $B_1 = -b_1^{(j)}$ are like $g(\tau) \sin(t/2)$ and have zero displacement at the top of the drive, maximum displacement at the bottom. In fact numerical evaluation shows, at least for $j = 1, 2, 3$, that $b_1^{(j)} < 0$, hence the cosine-mode instability boundary emanates from $B_{1/2,j}$ to the left, and the sine-mode to the right.

(e) *First harmonic resonance in the neighbourhood of $B = B_{1,j}$*

For this case set $B_0 = B_{1,j}$. The distinguished limit occurs on a timescale τ_2 and the solutions are independent of τ_1 . So, throughout this subsection, the solution depends on s, t , and $\tau \equiv \tau_2 = \epsilon^2 t$. The $O(\epsilon)$ solution (eq. (4.1)) is $T_1 = 0$ and

$$\mathbf{r}_1 = [f(\tau)\mathbf{m}_1 + g(\tau)\dot{\mathbf{m}}_1 + h(\tau)\mathbf{n}_1 + k(\tau)\dot{\mathbf{n}}_1] \phi(s),$$

where $\phi(s)$ is now a solution of

$$M_0\phi - \eta\phi \equiv B_{1,j}\phi^{IV} + L\phi - \eta\phi = 0, \quad (4.20)$$

subject to the usual boundary conditions. The amplitude functions $f(\tau)$, $h(\tau)$ and $g(\tau)$, $k(\tau)$ are to be determined. The unit vectors \mathbf{m}_n and \mathbf{n}_n , which rotate in the anti-clock-wise and clock-wise directions respectively about the \mathbf{k} axis, were defined in (4.13) and (4.14).

When this solution is substituted into the $O(\varepsilon^2)$ equation (4.2) the result is

$$\begin{aligned} \eta \frac{\partial^2 \mathbf{r}_2}{\partial t^2} + M_0 \mathbf{r}_2 - T_2' \mathbf{k} = \\ \frac{1}{2} \eta \left[\mathbf{i}(f+h) + \mathbf{j}(g-k) + f\mathbf{m}_2 + h\mathbf{n}_2 + \frac{1}{2}(g\dot{\mathbf{m}}_2 + k\dot{\mathbf{n}}_2) \right] L\phi - \\ B_{1,n} F(t, \tau) [(\phi'')^2]' \mathbf{k} - B_1 [f(\tau)\mathbf{m}_1 + g(\tau)\dot{\mathbf{m}}_1 + h(\tau)\mathbf{n}_1 + k(\tau)\dot{\mathbf{n}}_1] \phi^{IV}, \end{aligned} \quad (4.21)$$

where

$$F(t, \tau) = (f^2 + h^2 + g^2 + k^2) - 2(fk + hg) \sin 2t + 2(fh - gk) \cos 2t.$$

Also, by the inextensibility condition,

$$\mathbf{k} \cdot \mathbf{r}_2' = F(t, \tau) \Phi''(s) = -\frac{1}{2}(\mathbf{R}' \cdot \mathbf{R}'),$$

where $\Phi(s)$ satisfies the boundary-value problem (4.16). The tension T_2 is found to be given by (4.17) after $B_{1/2,j}$ is replaced by $B_{1,j}$.

The particular integral of equation (4.21) is

$$\begin{aligned} \mathbf{r}_2 = H_0(s) [f(\tau)\mathbf{m}_1 + g(\tau)\dot{\mathbf{m}}_1 + h(\tau)\mathbf{n}_1 + k(\tau)\dot{\mathbf{n}}_1] + F(t, \tau) \Phi'(s) \mathbf{k} + \\ H_1(s) [\mathbf{i}(f+h) + \mathbf{j}(g-k)] + H_2(s) \left[f\mathbf{m}_2 + h\mathbf{n}_2 + \frac{1}{2}(g\dot{\mathbf{m}}_2 + k\dot{\mathbf{n}}_2) \right] \end{aligned} \quad (4.22)$$

$$\text{where } M_0 H_0 + \eta H_0 = -B_1 \phi^{IV}, \quad M_0 H_1 = \frac{1}{2} \eta L \phi, \quad M_0 H_2 - 4\eta H_2 = \frac{1}{2} \eta L \phi. \quad (4.23)$$

For the first of these equations to have a solution, its right-hand side must be orthogonal to the eigenfunction of the operator on the left. Thus $B_1 = 0$, and without loss of generality $H_0(s) \equiv 0$.

When the above solutions are substituted into the right-hand side of the $O(\varepsilon^3)$ equation (4.3) the equation for the component \mathbf{u}_3 of \mathbf{r}_3 perpendicular to \mathbf{k} satisfies the equation

$$\begin{aligned} \eta \frac{\partial^2 \mathbf{u}_3}{\partial t^2} + M_0 \mathbf{u}_3 = \\ \mathbf{m}_1 \left\{ \frac{1}{2} \eta [LH_1(f+h) + LH_2 f] + (\phi' \mathcal{M} \Phi)' (f^2 + h^2 + g^2 + k^2) f + \right. \\ \left. [(\mathcal{M} \Phi - 4\eta \Phi) \phi']' [k(fk + hg) + h(fh - gk)] - B_2 \phi^{IV} f + 2\eta \phi \frac{dg}{d\tau} \right\} \\ + \text{similar terms in the directions } \dot{\mathbf{m}}_1, \mathbf{n}_1 \text{ and } \dot{\mathbf{n}}_1, \text{ and terms involving } \mathbf{m}_3 \text{ etc..} \end{aligned}$$

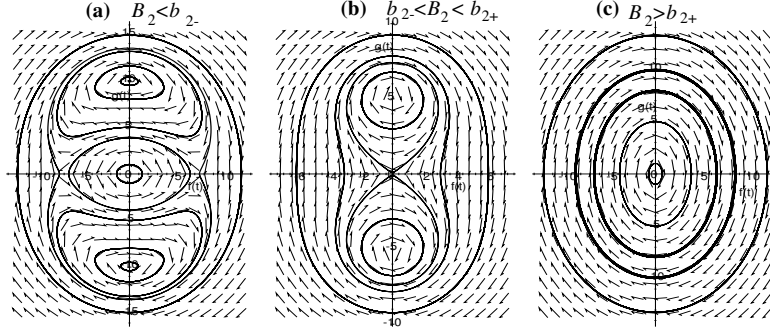


Figure 8. Phase portraits for solutions of the planar-mode amplitude equations (4.27) with $\eta = 60$ which implies $\alpha_2 = 19.46$, $\beta = 0.11635$ and $\gamma = -1.08504$. In (a) $B_2 = -10.32$, implying $\alpha_1 = 58.29$; (b) $B_2 = 5.05$, implying $\alpha_1 = -3.93$; (c) $B_2 = 20.16$, implying $\alpha_1 = -65.09$.

For a particular solution of this equation to exist the right-hand side must be orthogonal to the eigenfunction $\phi(s)$ of (4.20), which leads to the following amplitude equations for $f(\tau)$, $g(\tau)$, $h(\tau)$ and $k(\tau)$

$$\left. \begin{aligned} \frac{dg}{d\tau} + \alpha_1 f + \alpha_2 h - \beta(f^2 + h^2 + g^2 + k^2)f - \gamma(h^2 + k^2)f &= 0, \\ -\frac{df}{d\tau} + \alpha_1 g - \alpha_2 k - \beta(f^2 + h^2 + g^2 + k^2)g - \gamma(h^2 + k^2)g &= 0, \\ \frac{dk}{d\tau} + \alpha_1 h + \alpha_2 f - \beta(f^2 + h^2 + g^2 + k^2)h - \gamma(f^2 + g^2)h &= 0, \\ -\frac{dh}{d\tau} + \alpha_1 k - \alpha_2 g - \beta(f^2 + h^2 + g^2 + k^2)k - \gamma(f^2 + g^2)k &= 0, \end{aligned} \right\} \quad (4.24)$$

where

$$\left. \begin{aligned} \alpha_1 &= \int_0^1 \left[\frac{1}{2}\eta(LH_1 + LH_2) - B_2\phi^{IV} \right] \phi ds / \mathcal{B}, & \alpha_2 &= \int_0^1 \frac{1}{2}\eta LH_1 \phi ds / \mathcal{B}, \\ \beta &= \int_0^1 \mathcal{M}\Phi(\phi')^2 ds / \mathcal{B}, & \gamma &= \int_0^1 (\mathcal{M}\Phi - 4\eta\Phi) \phi'^2 ds / \mathcal{B}; & \mathcal{B} &= 2\eta \int_0^1 \phi^2 ds. \end{aligned} \right\} \quad (4.25)$$

The amplitude equations (4.24) may be expressed more simply in complex form via defining $u = f + ig$, $v = h + ik$:

$$\left. \begin{aligned} i\dot{u} &= \alpha_1 u + \alpha_2 \bar{v} - \beta(|u|^2 + |v|^2)u + \gamma|v|^2 u, \\ i\dot{v} &= \alpha_1 v + \alpha_2 \bar{u} - \beta(|v|^2 + |u|^2)v + \gamma|u|^2 v, \end{aligned} \right\} \quad (4.26)$$

where an overbar represents complex conjugation.

Like the simpler amplitude equations (4.10), the ‘normal form’ (4.26) is completely integrable and circularly symmetric. There also exist relative equilibria solutions, which in this case correspond to a slow-time rotational drift of the fast-time planar oscillations. A detailed analysis of this normal form is left for future work. We shall restrict ourselves here to the simplest class of solutions, namely the planar modes, which, without loss of generality, we shall assume to lie in the (\mathbf{i}, \mathbf{k}) -plane. Hence, setting $h = f$ and $k = g$ equations (4.24) become

$$\left. \begin{aligned} \frac{dg}{d\tau} &= -[(\alpha_1 + \alpha_2) - (2\beta + \gamma)(f^2 + g^2)] f, \\ \frac{df}{d\tau} &= [(\alpha_1 - \alpha_2) - (2\beta + \gamma)(f^2 + g^2)] g, \end{aligned} \right\} \quad (4.27)$$

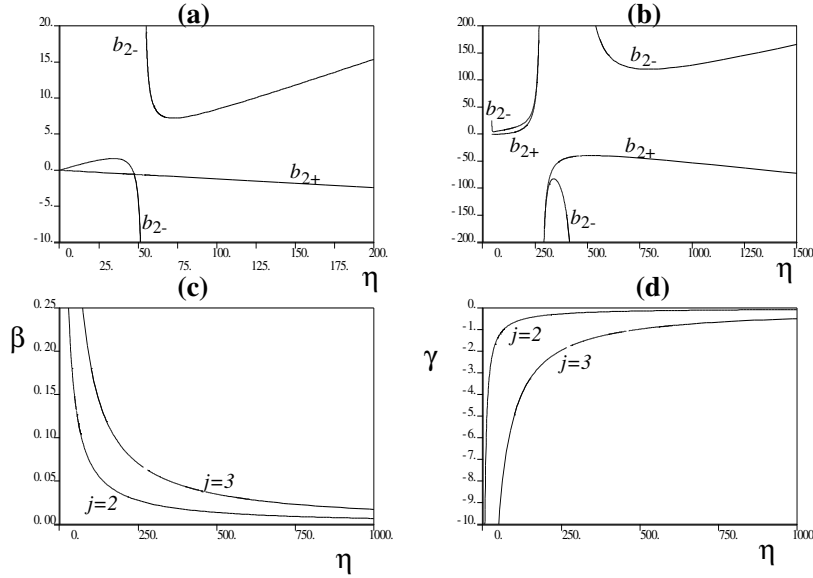


Figure 9. Numerically calculated coefficients (4.25) for $B = B_1$, j with $j = 2, 3$. (a) and (b) depict the B_2 -values $b_{2\pm}(\eta)$ at which $\alpha_1 = \pm\alpha_2$ for $j = 2, 3$ respectively. (c) and (d) depict $\beta(\eta)$ and $\gamma(\eta)$.

the stationary equilibrium points of which are

$$f = g = 0; \quad f = \pm \sqrt{\frac{\alpha_1 + \alpha_2}{2\beta + \gamma}}, \quad g = 0; \quad \text{and} \quad f = 0, \quad g = \pm \sqrt{\frac{\alpha_1 - \alpha_2}{2\beta + \gamma}}.$$

It is straightforward to show that the only possible equilibria to the full system (4.26) are trivial rotations of these.

Note also that a linear stability analysis about the trivial equilibrium shows that the boundary between stability and instability is given by $\alpha_1 = \pm\alpha_2$ with stability occurring for $|\alpha_1| < |\alpha_2|$. Figure 8 plots representative phase portraits for just the planar modes (solutions to (4.27)) using numerical evaluation of the coefficients (4.25). Note that a pair of stable $g = 0$ non-trivial equilibria are born for $B_2 < b_{2+}$ which correspond to lateral vibrations of the column that are out of phase with the drive (‘snaking’). For $B_2 < b_{2-}$ there is also a pair of unstable $f = 0$ equilibria corresponding to vibrations in phase with the drive (‘nodding’).

Finally, it remains to see how α_1 , α_2 , β , γ and $B_2 = b_{2\pm}^{(j)}$ defining the stability boundaries $\alpha_1 = \pm\alpha_2$, all depend on η . These loci were obtained by numerical computation of the boundary-value problems (4.22) using AUTO, and subsequent evaluation of the integrals (4.25). The results are plotted in Figure 9 for $j = 2$ and $j = 3$. Note the singularities in the coefficients $b_{2-}^{(2)}$ and $b_{2-}^{(3)}$ which detailed numerics reveal to occur at $\eta = 53.3$ and 460.7 respectively. Also both coefficients $b_{2\pm}^{(j)}$ become singular for $\eta \approx 279$. Meanwhile $\beta > 0$ and $\gamma < 0$ always.

Note how the singularities of $b_{2-}^{(j)}$ (the high- η one in the case $j = 3$) occur at precisely the η -values as those of the coefficient b_2 of the falling-over instability; see Figure 4. An examination of the curves $B_{2,j}(\eta)$ (see Table 1 in Part I) reveals that these are precisely the η -values at which $B_{1,j} = B_{0,1}$, i.e. there is a resonance tongue

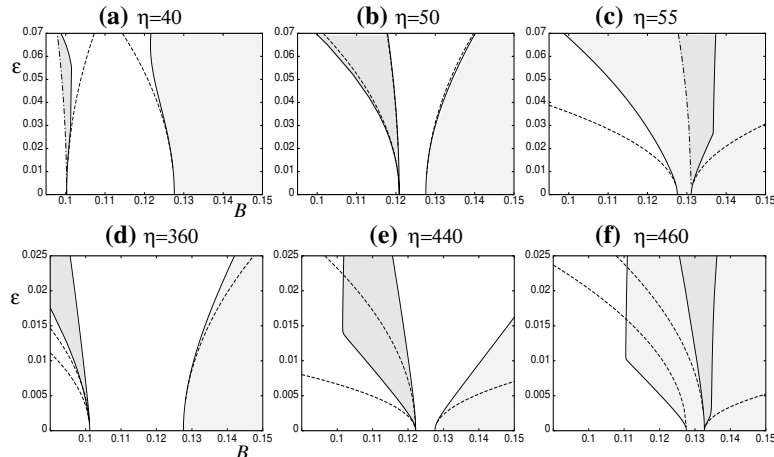


Figure 10. Resonance tongue interaction in the (B, η) -plane between the the falling over instability emanating from $B = B_{cr} = 0.127954$ and (a)–(c) the tongue emanating from $B_{1,2}$, (d)–(f) the tongue from $B_{1,3}$. Solid lines are from the two-timescale asymptotics, dashed lines from the Floquet-theory numerics and dot-dashed lines are where the two curves are overlaid. Light shading represents the primary stability region to the right of the numerical falling over boundary, and dark shading gives the instability region inside the $B_{1,n}$ tongue.

interaction between the falling-over mode and the harmonic resonance. Figure 10 shows how the asymptotic theory is matched by the numerical Floquet analysis (with $N = 4$) in describing this curious interaction process.

5. Discussion

In this paper we have extended our earlier analysis of the ‘Indian rope trick’ to include both geometric nonlinearity and a careful asymptotic description of the simplest static bifurcations and dynamic resonances. At each resonance we have derived the appropriate amplitude equations which resemble normal forms for bifurcations in nonlinear wave systems with symmetry (e.g. Dangelmayr et al. (1996)). A complete analysis of these normal forms, especially the dynamics associated with fully three-dimensional motions of the column, is left for future work. The main insights in this paper have concerned simply the linear instability criteria that can be deduced from these normal forms, especially how the quadratic coefficients of resonance tongues in the (B, ε) -plane becomes singular at η -values corresponding to a mode interaction between the pure falling over instability and the resonance between a vibration mode and the drive frequency (as in Figure 10). The subharmonic instability analysed in §4(d) is less interesting in this regard because, as illustrated in Figure 7, this linear-to-first-order tongue is not affected by its crossing B_{cr} .

Let us now comment from the asymptotic analysis why the resonance tongue interaction occurs when $B_{1,j}$ crosses B_{cr} . Consider equation (4.8)₂ that determines the function F_1 used in the evaluation of the falling-over instability tongue. It can be solved provided the operator on the left-hand side is invertible. However, at precisely the η -value $\eta_{1,j}$, say, for which $B_0 = B_{1,j}$, then by definition η is an eigenvalue of M_0 , and hence the operator is not invertible. Thus the asymptotic

expansion breaks down as $\eta \rightarrow \eta_{1,j}$ and hence F_1 blows up. Hence the coefficient b_2 defined by $P = 0$ blows up also, which explains the singularities in the curve $b_2(\eta)$ plotted in Figure 4 at $\eta = 53.3, 460.7$ and 1813.5 , where $B_0 = B_{1,j}$ for $j = 1, 2, 3$ respectively. A similar reasoning applied to the middle equation of (4.23) shows that H_1 blows up as $\eta \rightarrow \eta_{1,j}$ and hence, from (4.25), the coefficient b_{2-} corresponding to $\alpha_1 = -\alpha_2$ blows up also. This then explains the seemingly strange interactions of the stability boundaries shown in Figure 10 for η near $\eta_{1,2}$ and $\eta_{1,3}$.

The details of Tom Mullin’s experiments will be written up elsewhere (Acheson et al. 2000). Let us here make just two remarks on how the present theory appears highly promising at least at a qualitative level. First, the experimentally observed lower stability boundary in the (B, η) -plane for fixed ε is in the vicinity of $\eta = \eta_{1,3}$. Hence, the resonance tongue interaction just described seems absolutely crucial in explaining the quantitative inaccuracy of the simple formula given in Part I. Second, the two instabilities seen in the experiment do indeed correspond to a pure falling over mode and something corresponding to the ψ_3 spatial mode oscillating at the frequency of the drive, which is fully consistent with the hypothesis that it is the interaction between these two modes for $\eta \approx \eta_{1,3}$ that underlies what is observed.

When trying to match the experiments on curtain wire, however, it should be remembered that the analysis presented here contains no damping. As is well known (e.g. Nayfeh & Mook (1979)), damping will lift those resonance tongues corresponding to higher harmonics away from the $\varepsilon = 0$ axis. In some sense, this justifies the concentration in this paper on only the lowest order resonance tongues. Future work will be directed towards including a realistic material damping term into the model, in the first instance by considering the column as the limit of N pendulums coupled by rotational springs and dampers. Also, one strange feature of curtain wire is that it is clearly not linearly elastic. In fact, the softening nonlinearity in its bending moment constitutive law (essentially due to the spring coils opening up as they are bent) is so extreme that its static buckling is subcritical (see, the results by T.B. Benjamin reproduced in (Iooss & Joseph 1990, p.22-24)). However, the analysis in §3 above shows that linearly elastic columns buckle supercritically due to the effect of purely geometric nonlinearities. While this observation may seem to belittle a lot of the analysis in this paper, one should remember that the stability curves are defined by the purely linear problem. Also, Tom Mullin has performed other experiments which have demonstrated that linearly elastic columns such as those made of niobium wire can also be stabilized by parametric excitation. It just seems that the curtain wire gives the most repeatable results for resonance tongue boundaries — perhaps because it has high damping and hence is least influenced by higher-order resonances.

Acknowledgements

The work of WBF was supported by an EPSRC Visiting Fellowship at Bristol and an Australian Research Council Large Grant The work of ARC was supported by the EPSRC with whom he holds an Advanced Fellowship. We should like to thank Tom Mullin (University of Manchester) for showing us his experimental results ahead of publication, and Jorge Galan (University of Sevilla) and David Acheson (Jesus College, Oxford) for stimulating discussions.

References

- Acheson, D. (1993), 'A pendulum theorem', *Proc. Roy. Soc. Lond. A* **443**, 239–245.
- Acheson, D. (1995), 'Multiple-nodding oscillations of a driven inverted pendulum', *Proc. Roy. Soc. Lond. A* **448**, 89–95.
- Acheson, D. (1997), *From Calculus to Chaos, An Introduction to Dynamics*, Oxford University Press, Oxford.
- Acheson, D. & Mullin, T. (1993), 'Upside-down pendulums', *Nature* **366**, 215–216.
- Acheson, D., Champneys, A., Fraser, W., Galan, J. & Mullin, T. (2000), 'Stabilizing a wire upside down by parametric excitation'. In preparation.
- Champneys, A. & Fraser, W. (2000), 'The 'indian rope trick' for a continuously flexible rod; linearized analysis', *Proc. Roy. Soc. Lond. A* **456**, 553–570.
- Dangelmayr, G., Fiedler, B., Kirchgässner, K. & Mielke, A. (1996), *Dynamics of nonlinear dissipative systems: reduction, bifurcation and stability*, Longman, Harlow, U.K. Pitman Research Notes in Mathematics Series, no. 352.
- Doedel, E., Champneys, A., Fairgrieve, T., Kuznetsov, Y., Sandstede, B. & Wang, X. (1997), 'AUTO97 continuation and bifurcation software for ordinary differential equations'. Available by anonymous ftp from FTP.CS.CONCORDIA.CA, directory PUB/DOEDEL/AUTO.
- Greenhill, A. (1881), 'Determination of the greatest height consistent with stability that a pole or mast can be made . . .', *Proceedings of the Cambridge Philosophical Society* **IV** Oct 1880 – May 1883, 65–73.
- Iooss, G. & Joseph, D. (1990), *Elementary stability and bifurcation theory*, second edn, Springer-Verlag, New York.
- Kevorkian, J. & Cole, J. (1981), *Perturbation methods in applied mathematics*, Springer-Verlag, New York.
- Nayfeh, A. & Mook, D. (1979), *Nonlinear Oscillations*, Wiley Interscience, New York.
- Otterbein, S. (1982), 'Stabilisierung des n-pendels und der indische seiltrick', *Arch. Rat. Mech. Anal.* **78**, 381–393.
- Stephenson, A. (1908), 'On a new type of dynamical stability', *Mem. Proc. Manch. Lit. Phil. Soc.* **52**, 1–10.
- Weibel, S. & Baillieul, J. (1998), 'Open-loop oscillatory stabilization of an n -pendulum', *Int. J. Control* **71**, 931–957.